crystals

MDPI

Article

Inhibition of the Alkali-Carbonate Reaction Using Fly Ash and the Underlying Mechanism

Xin Ren, Wei Li, Zhongyang Mao and Min Deng *

College of Materials Science and Engineering, Nanjing Tech University. Nanjing 210009, China; 201761100171@njtech.edu.cn (X.R.); 201762100015@njtech.edu.cn (W.L.); mzy@njtech.edu.cn (Z.M.)
* Correspondence: dengmin@njtech.edu.cn; Tel.: +86-159-5059-1582

Received: 10 May 2020; Accepted: 3 June 2020; Published: 5 June 2020

Abstract: In this paper, fly ash is used to inhibit the alkali-carbonate reaction (ACR). The experimental results suggest that when the alkali equivalent (equivalent Na_2Oeq) of the cement is 1.0%, the adding of 30% fly ash can significantly inhibit the expansion in low-reactivity aggregates. For moderately reactive aggregates, the expansion rate can also be reduced by adding 30% of fly ash. According to a polarizing microscope analysis, the cracks are expansion cracks mainly due to the ACR. The main mechanisms of fly ash inhibiting the ACR are that it refines the pore structure of the cement paste, and that the alkali migration rate in the curing solution to the interior of the concrete microbars is reduced. As the content of fly ash increases, the concentrations of K^+ and Na^+ and the pH value in the pore solution gradually decrease. This makes the ACR in the rocks slower, such that the cracks are reduced, and the expansion due to the ACR is inhibited.

Keywords: inhibit; alkali-carbonate reaction; fly ash; expansion; mechanism

1. Introduction

In 1940, Stanton [1] first discovered the alkali-aggregate reaction (AAR), which has attracted the attention of many researchers. As it is extremely destructive and difficult to repair, it has been called the "cancer" of concrete. The AAR is divided into alkali-silicate reactions (ASRs) and alkali-carbonate reactions (ACRs). The ACR is one of the main problems in the long-term durability of concrete.

According to the time sequence, the expansion mechanism of the ACR can be divided into three types. Firstly, Gillott [2] believed that the expansion is the result of an increase in the solid volume due to water absorption by the clay, where dolomitization only provides a way for clay to absorb water. Secondly, Tang and Tong [3–5] believed that, although the absolute volume of the solid phase of the alkali-dolomite reaction is reduced in theory, the rearrangement and crystallization of the reaction products in a restricted space causes the expansion and cracking of the aggregate, respectively, leading to concrete cracking. Thirdly, Katayama [6–8] believed that the ACR is the combination of harmful expansion caused by the ASR of microcrystalline quartz and harmless dolomitization. Dolomitization produces the brucite and carbonate reaction ring, but the expansion is caused by the ASR due to microcrystalline quartz. However, Chen, X [9] and Chen, B [10] used tetramethylammonium hydroxide (TMAH) as the curing solution to investigate the expansion characteristics caused only by the ACR, as TMAH does not react with SiO_2. Their results showed that the ACR exists separately and contributes to the expansion. Huan Yuan [11], who also used TMAH as the curing solution, proved (by an expansion stress test and concrete microbar expansion test) that the alkali-carbonate reaction causes expansion.

The concrete durability problem caused by the AAR can be controlled by many methods, such as reducing the available alkali and adding a suitable amount of ash or chemical additives [12]. Supplementary cementitious materials (SCMS) have different effects in reducing the expansion due to

the ACR and ASR [13]. It is well-known that supplementary cementitious materials have a significant effect in inhibiting the ASR [14]. Based on the success of these materials, they have been used to prevent the deterioration caused by the ACR. According to the research of Alireza Joshaghani [15], fly ash and trass can reduce the expansion rate of the ACR. At 56 d, using 10%, 20%, and 30% fly ash can reduce the expansion rate of mortar bars by 47%, 95%, and 73%, respectively, according to the ASTM C1260 standard. According to the experimental results of concrete prisms, the inhibitory effect of trass on the ACR is slightly better than that of fly ash. In a long-term test, the optimal content of fly ash was 20% and the optimal content of trass was 30%. Shehata's [16] experiment demonstrated that the expansion of concrete prisms mixed with SCMs exceeded the threshold of 0.040% in two years and no SCM had a complete effect on the ACR in the long-term, although some types were more effective than others at reducing expansion.

Shehata [16] and Min Deng [17] have shown that using fly ash to effectively inhibit the ACR expansion of the highly reactive dolomite limestones from Kingston, Canada is difficult. However, whether the ACR of low-reactive dolomite rocks and moderately reactive dolomite rocks can be effectively inhibited has not yet been studied. At present, the related specifications stipulate that concrete works cannot use the ACR reactive rocks as aggregates, limiting the application of dolomite rocks. Research on fly ash on the ACR of low-reactive dolomite rocks and moderately reactive dolomite rocks is therefore necessary. This serves to play a guiding role in the engineering application of dolomitic aggregates.

The main purpose of this study is to examine the inhibition and mechanism of fly ash on the ACR. Although the impact of fly ash on the ASR has been well-documented, there has been little research on the impact of fly ash on the ACR. In addition, most of the studies have focused on highly reactive aggregates, such as the Kingston dolomite limestone of Canada, with no clear research on low-reactive and moderately reactive rocks. In this study, therefore, we focus on low- and moderately reactive dolomite rocks.

2. Materials and Methods

2.1. Materials

The used materials were (1) low-alkali Portland cement (Type II) obtained from the Jiangnan Cement Plant, Nanjing, China, with 0.54% equivalent Na_2Oeq; (2) class F fly ash (FA) obtained from Henan; and (3) dolomitic limestones obtained from Baofuling Mountain, Shandong, China (BFL8) and Shuijingwan, Guizhou, China (SJW). The chemical compositions of the cement and fly ash are presented in Table 1. The chemical compositions of the dolomitic limestones are shown in Table 2.

Table 1. Chemical analysis of cement and fly ash (wt. %).

Samples	Chemical Compositions (wt. %)								
	SiO_2	CaO	MgO	Al_2O_3	Fe_2O_3	SO_3	K_2O	Na_2O	LOI
Cement (Type II)	22.02	60.51	2.18	6.34	3.05	1.86	0.47	0.23	1.96
Fly Ash	48.91	5.01	1.03	34.18	5.22	1.20	0.89	0.39	1.05

Table 2. Chemical analysis of aggregates (wt. %).

Samples	Chemical Compositions (wt. %)					
	SiO_2	CaO	MgO	Al_2O_3	Fe_2O_3	LOI
BFL8	2.68	48.65	4.39	0.93	0.26	42.06
SJW	7.68	42.68	5.21	1.26	0.88	38.64

The microscopic appearances of the fly ash and cement observed with a scanning electron microscope (SEM; JSM-6510, JEOL Co, Tokyo, Japan) are shown in Figure 1. The fly ash is shown in (A)

and the cement is shown in (B). We can see, from Figure 1, that the fly ash particles were rounded and most particles in the cement were irregularly shaped. The X-ray diffraction (XRD; SmartLab X-ray diffractometer, Rigaku Co., Tokyo, Japan) analysis results are shown in Figure 2. The XRD analysis of SJW is shown in (A) and BFL8 is shown in (B). SJW rocks mainly include calcite, quartz, dolomite and muscovite. However, BFL8 rocks only have calcite, quartz and dolomite.

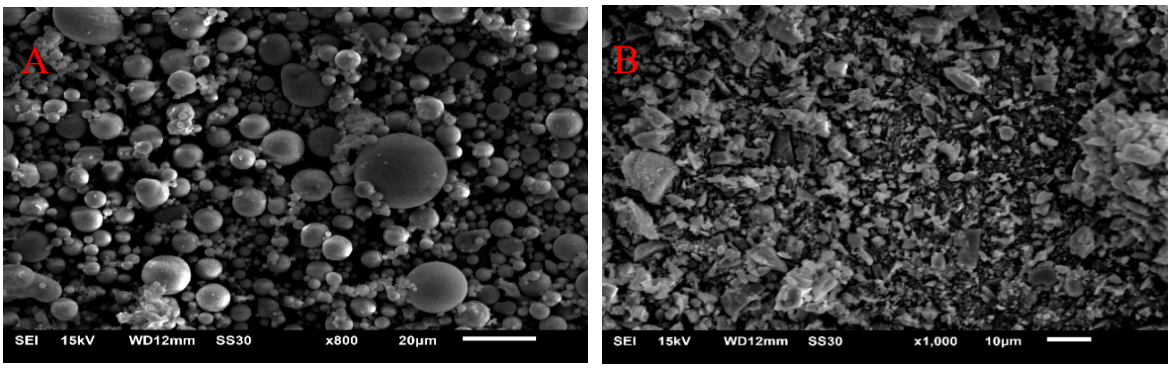

Figure 1. Scanning electron microscope images of (**A**) fly ash and (**B**) cement.

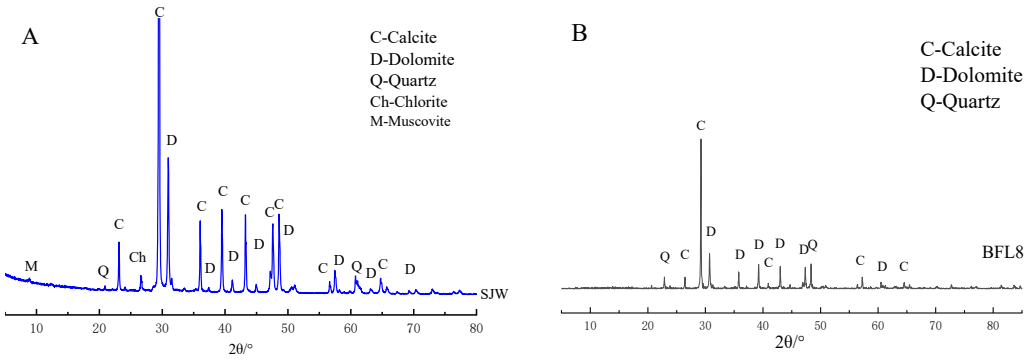

Figure 2. XRD analysis of (**A**) SJW and (**B**) BFL8.

2.2. Methods

2.2.1. Mortar Bars Test

A set of mortar bars (25 × 25 × 285 mm) were prepared with cement as well as dolomitic rocks with grain sizes of 0.125–4 mm, according to RILEM AAR-2 [18]. The alkali equivalent (equivalent Na_2Oeq) of the cement was adjusted to 0.9%, the ratio of aggregate to cement was 1:1, and the water–cement ratio was adjusted to 0.32. The designs of the mortar bars, according to RILEM AAR-2, are shown in Table 3. All specimens were kept for 24 h in a moisturized condition for curing before demolding. Then, samples were transferred to 1 mol/L NaOH solution immediately and stored in sealed containers at 80 °C. When curing to a set age, remove the sample and measure the length, then calculate the expansion rate according to Equation (1):

$$P_t = (L_t - L_0)/(L_0 - 2b) \times 100\% \quad (1)$$

where P_t is the expansion rate after t days of curing, in %; L_t is the test piece length after t days of curing, in mm; L_0 is the initial length of the test piece, in mm; and b is the length of the nail embedded in the concrete, in mm.

Table 3. Mortar bars mix designs according to RILEM AAR-2.

Sample Name	w/c	Cement/g	Aggregates/g
BFL8-1	0.47	400	900
SJW-1	0.47	400	900

2.2.2. Concrete Microbars Test

A set of concrete microbars (40 × 40 × 160 mm) were prepared with cement, as well as dolomitic rocks with grain sizes of 5–10 mm, according to RILEM AAR-5 [19]. The alkali equivalent (equivalent Na_2Oeq) of the cement was adjusted to 1.5%. The ratio of aggregate to cement was 1:1, and the water–cement ratio was adjusted to 0.32. The designs of the microbars, according to RILEM AAR-5, are shown in Table 4. All specimens were kept for 24 h in a moisturized condition for curing before demolding. Then, samples were transferred to 1 mol/L NaOH solution immediately and stored in sealed containers at 80 °C. The expansion rate is calculated according to Equation (1).

Table 4. Concrete microbars mix designs according to RILEM AAR-5.

Sample Name	w/c	Cement/g	Fly Ash/g	Aggregates/g
BFL8-2-FA0%	0.32	900	0	900
BFL8-2-FA10%	0.32	810	90	900
BFL8-2-FA20%	0.32	720	180	900
BFL8-2-FA30%	0.32	630	270	900
SJW-2-FA0%	0.32	900	0	900
SJW-2-FA10%	0.32	810	90	900
SJW-2-FA20%	0.32	720	180	900
SJW-2-FA30%	0.32	630	270	900

2.2.3. Concrete Prisms Test

A set of concrete prisms were prepared with cement, as well as dolomitic rocks with grain sizes of 4.75–19 mm, according to ASTM C1293 [20]. The alkali equivalent (equivalent Na_2Oeq) of the cement was adjusted to 1.25%. The water–cement ratio was adjusted to 0.45. The designs of the concrete prisms, according to ASTM C1293, are shown in Table 5. All specimens were kept for 24 h in a moisturized condition for curing before demolding. Then, samples were transferred to 100% humidity at 38 °C. The expansion rate is calculated according to Equation (1).

Table 5. Concrete prisms mix designs according to ASTM C1293.

Sample Name	w/c	Cement/g	Fly Ash/g	Aggregates/g	Sand/g
BFL8-3-FA0%	0.45	3360	0	6000	3980
BFL8-3-FA30%	0.45	2352	1008	6000	3980
SJW-3-FA0%	0.45	3360	0	6000	3980
SJW-3-FA30%	0.45	2352	1008	6000	3980

2.2.4. Measurement of the PH, Ionic Concentration and Pore Structure

Three sets of samples (20 × 20 × 20 mm) were prepared with cement and fly ash, where the cement was replaced with varying amounts of fly ash. The samples were separately cured in a 1 mol/L NaOH solution and saturated $Ca(OH)_2$ solution at 80 °C. First, to determine the curing age, 5.0 g of cement paste was weighed. Second, the contents were transferred to a covered dish and broken up. Third, enough water was added to make up a volume of 200 ml. Fourth, the mixture was incubated at room temperature for 1 h, and stirred frequently. Then, the mixture was filtered with medium-quality filter paper into a 500 ml volumetric flask and washed with hot water. Finally, the K^+ and Na^+ concentrations of the pore solution were measured with a flame photometer (FP650, Aopu Co.

Shanghai, China) and the pH value of the pore solution was measured with a pH meter (PHS-25, INESA Co. Shanghai, China).

Three sets of samples (20 × 20 × 20 mm) were prepared with cement and fly ash. The water–cement ratio was adjusted to 0.32. They were separately cured in 1 mol/L NaOH solution at 80 °C. To determine the curing age, the cement paste was taken and the porosity and pore size distribution were measured using mercury intrusion porosimetry (MIP, AutoPore W 9500, Micromeritics Co. New York, NY, USA). As shown in Table 6, four mix formulations of cement pastes were designed to comparatively investigate the influences of fly ash on the pH, ionic concentration, and pore structure of the cement pastes.

Table 6. Mix proportions of the cement pastes.

Sample Name	w/c	Cement/g	Fly Ash/g
FA-0%	0.32	450	0
FA-10%	0.32	405	45
FA-20%	0.32	360	90
FA-30%	0.32	315	135

2.2.5. Thin Section Petrography

Samples taken from the concrete microrods were cut into thin slices. Then, the slices were examined with an optical microscope to check for the presence of reaction products and expansion cracks derived from the aggregate. A polarized optical microscope with transmitted light (Optiphot-II Pol reflectometer, × 25–400, Nikon, Tokyo, Japan) and a stereomicroscope (BH-2, Nikon, Tokyo, Japan) were used for this purpose. The preparation of thin sections was carried out according to the "Thin section specimen preparation" section in [21].

3. Results and Discussion

3.1. Discrimination of the Aggregate Alkali Reactive

The results of the mortar bar test (according to RILEM AAR-2) and concrete microbar test (according to RILEM AAR–5) are shown in Figures 3 and 4, respectively.

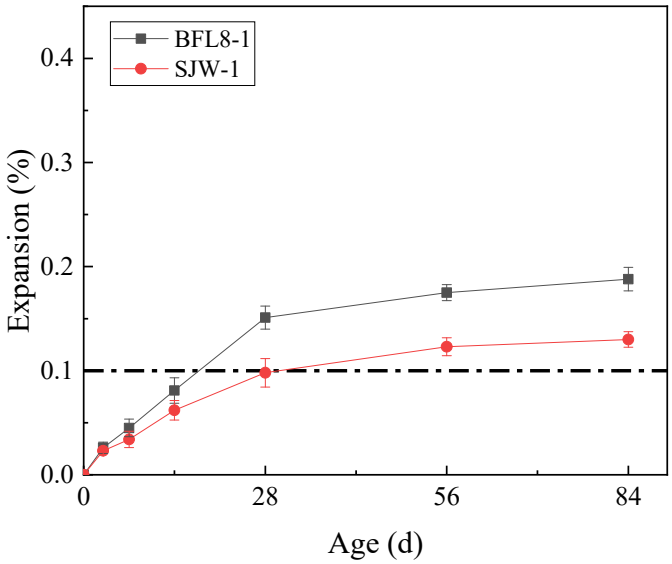

Figure 3. The expansion of the mortar bars prepared according to RILEM AAR-2.

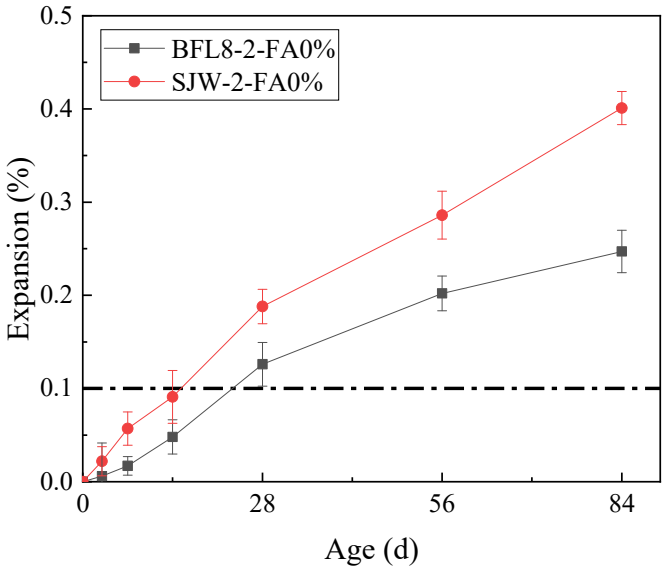

Figure 4. The expansion of the concrete microbars prepared according to RILEM AAR-5.

Figure 3 shows that the expansion of BFL8 and SJW at 28 d was 0.126% and 0.188%, respectively. At 28 d, their expansion was greater than 0.1%, which is indicated by the position of the dotted line in the figure. According to RILEM AAR-5, the aggregates of BFL8 and SJW both demonstrated alkali-carbonate reactions.

Figure 4 shows that the expansion of BFL8 and SJW at 14 days was 0.081%, 0.062%, respectively. The dotted line in Figure 4 is the threshold value for judging whether the aggregate demonstrates an alkali–silicate reaction. At 14 d, the expansions of BFL8 and SJW were less than 0.1%; therefore, according to RILEM AAR-2, the BFL8 and SJW aggregates had no alkali-silicate reactions

Based on Figures 3 and 4, we can see from the expansion rate that BFL8 has low reactivity and SJW has moderate reactivity. Furthermore, BFL8 and SJW only have alkali-carbonate reactions.

3.2. The Effect of Fly Ash on Concrete Microbars in the Short Term

3.2.1. Alkali Equivalent (Equivalent Na_2Oeq) of the Cement Adjusted to 1.5%

Figure 5 shows the expansion results of the 180-day concrete microbar test conducted on samples using different concentrations of fly ash, according to RILEM AAR-5, where the alkali equivalent (equivalent Na_2Oeq) of the cement was adjusted to 1.5%. The expansion of concrete microbars prepared by BFL8 is shown in (A) and the expansion of concrete microbars prepared by SJW is shown in (B).

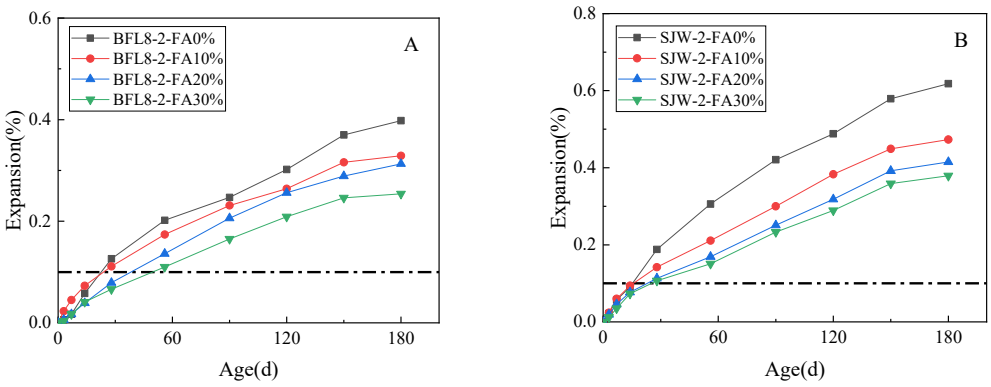

Figure 5. The expansion of the concrete microbars with fly ash: (**A**) concrete microbars prepared by BFL8 and (**B**) concrete microbars prepared by SJW.

Figure 5 shows that the expansion rates of BFL8 and SJW without fly ash were 0.126% and 0.188%, respectively, at 28 days. The BFL and SJW samples expanded about 0.398% and 0.618%, respectively, at 180 days. Compared with the concrete microbars mixed with 0% fly ash, the expansion of the concrete microbars mixed with 10%, 20%, and 30% fly ash and prepared with BFL8 decreased by 18%, 42%, and 51%, respectively, at 28 d, and by 17 %, 21%, and 36%, respectively, at 180 d. The expansion of the concrete microbars mixed with 10%, 20%, and 30% fly ash and made of SJW decreased by 29%, 43%, and 46%, respectively, at 28 d, and by 23%, 33%, and 39%, respectively, at 180 d. After curing in 80 °C 1 mol/L NaOH solution for 56 days, the expansion of the concrete microbars prepared with BFL8 mixed with 10%–30% fly ash was greater than 0.10%. After curing for 28 days in 1mol/L NaOH solution, the expansion of the concrete microbars prepared with SJW mixed with 10%–30% fly ash was greater than 0.10%. From this point of view, when the alkali equivalent (equivalent Na_2Oeq) of the cement is 1.5%, 10%–30% fly ash cannot effectively inhibit the expansion of the low-reactivity BFL8 and the moderately reactive SJW.

3.2.2. Alkali Equivalent (Equivalent Na_2Oeq) of the Cement Adjusted to 1.0%

When the alkali equivalent (equivalent Na_2Oeq) of the cement was 1.5%, fly ash could not effectively inhibit the ACR. Therefore, we reduced the alkali equivalent (equivalent Na_2Oeq) of the cement to study the effect when the alkali equivalent (equivalent Na_2Oeq) of the cement was 1.0%, in order to determine whether fly ash can effectively inhibit the expansion caused by the ACR under such conditions.

Figure 6 shows the expansion results of a 240-day concrete microbar test conducted on samples using different concentrations of fly ash according to RILEM AAR-5, where the alkali equivalent (equivalent Na_2Oeq) of the cement was 1.0%. The expansion of concrete microbars prepared by BFL8 is shown in (A) and the expansion of concrete microbars prepared by SJW is shown in (B).

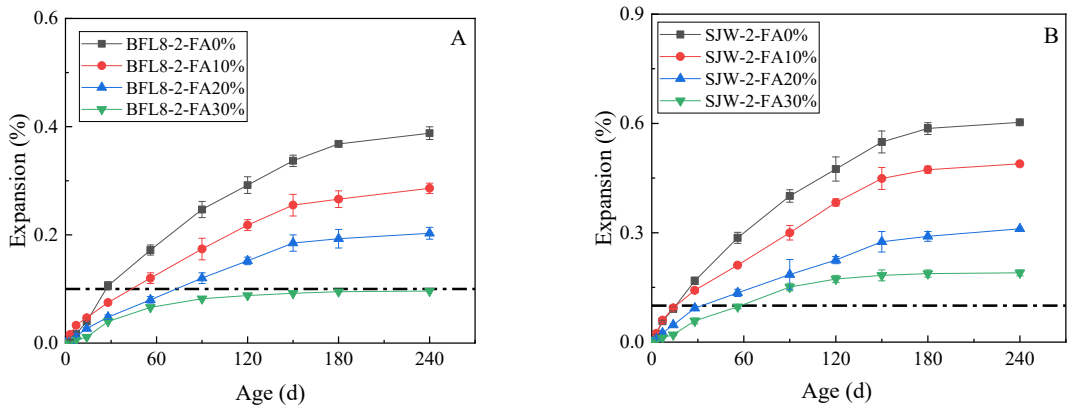

Figure 6. The expansion of the concrete microbars with fly ash: (**A**) concrete microbars prepared by BFL8 and (**B**) concrete microbars prepared by SJW.

Figure 6 shows that the expansion rates of BFL8 and SJW without fly ash were 0.106% and 0.168%, respectively, at 28 days. These samples of BFL8 and SJW expanded by approximately 0.388% and 0.603%, respectively, at 240 days, and their expansion basically stabilized. As the content of fly ash increased, the expansion of the concrete microbars made of BFL8 and SJW gradually decreased. At 28 d and 240 d, the addition of 10%, 20%, and 30% fly ash reduced the expansion of the concrete microbars prepared with BFL8 by 35%–66% and 26%–75%, respectively. Furthermore, adding 10%, 20%, and 30% fly ash reduced the expansion of the concrete microbars prepared with SJW by 16%–66% and 19%–67%, respectively.

Based on Figure 6, we can see, from the expansion rate, that adding 10%, 20%, and 30% fly ash reduced the expansion. However, when adding 30% fly ash, the expansion of SJW still exceeded 0.1%

at 90 d. For BFL8, when the alkali equivalent (equivalent Na_2Oeq) of the cement was 1.0%, adding 30% fly ash controlled the expansion within 0.1%.

3.3. The Effect of Fly Ash on Concrete Microbars in the Long-Term

The expansion results of the one-year concrete prisms test conducted on samples using 30% fly ash according to ASTM C1293 are shown in Figure 7, which shows that fly ash reduced the expansion for all tested aggregates.

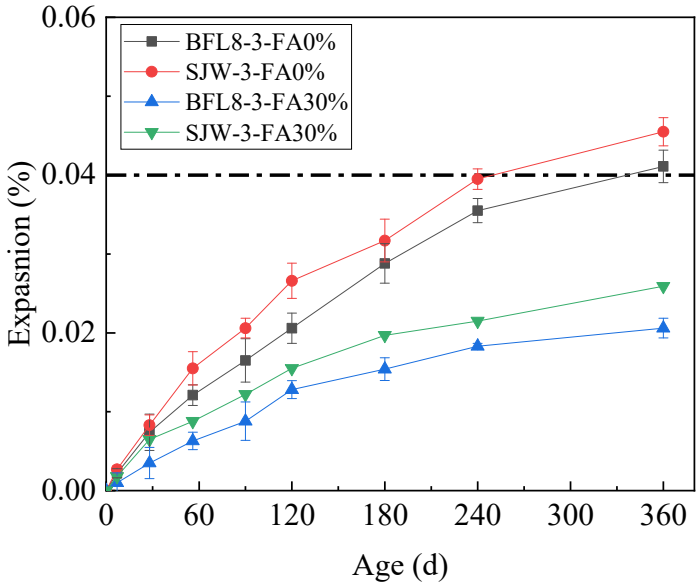

Figure 7. The expansion of the concrete prisms with fly ash.

Figure 7 shows that the expansion rates of BFL8 and SJW without fly ash were equal to 0.041% and 0.046%, respectively, at 360 days. In accordance with the expansion of the concrete prisms with 30% fly ash, using fly ash reduced the expansion due to the ACR, and thus the expansion rates of BFL8 and SJW decreased by 49% and 43%, respectively. The expansion of the concrete prisms prepared with 30% FA and made of BFL8 and SJW were 0.0206% and 0.0259%, respectively, at 360 d. The expansion rates of the concrete prisms were less than 0.040%. Therefore, adding 30% fly ash can effectively reduce the expansion rate due to the ACR.

3.4. The Mechanism of Fly Ash Inhibiting ACR

3.4.1. The Effect of Fly Ash on PH Value

The pH value of the cement paste pore solution cured in saturated $Ca(OH)_2$ at 80 °C for 28 days is shown in Figure 8, which indicates that fly ash can significantly reduce the pH value of the pore solution and delay the ACR reaction. The ACR reaction requires a pH value of 12, according to Tang and Den [22].

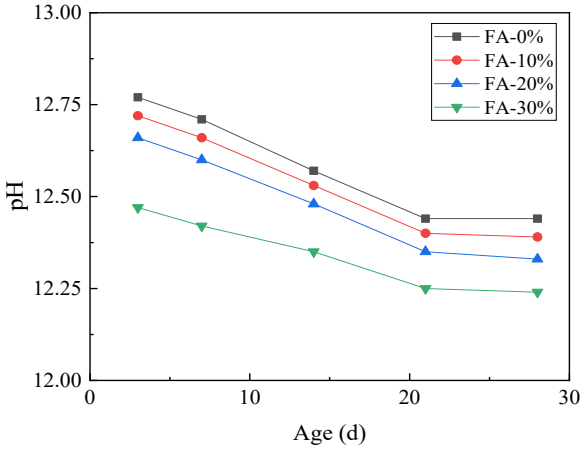

Figure 8. The influence of fly ash on pH in the cement paste pore solution (80 °C, $Ca(OH)_2$).

Adding 30% fly ash significantly decreased the pH value of the pore solution. Based on Figure 8, the pH value of the cement paste pore solution without fly ash was 12.45, and the pH of the cement paste pore solution with 30% fly ash was 12.25 at 21 days. Many researchers [23] have asserted that the concentration of OH^- plays an important role in the ACR and that reducing the concentration of OH^- can reduce the damage to the aggregates and inhibit the ACR.

The main reason why fly ash reduces the pH is because it plays the role of a physical diluent and reduces the alkali concentration of the pore solution [13,24]. Over the long-term, the fly ash reacts with $Ca(OH)_2$ to reduce the pH value.

3.4.2. The Effect of Fly Ash on the Ionic Migration and Pore Structure

Figure 9 shows the influence of fly ash on the concentrations of K^+ and Na^+ in the pore solution after curing in 1 mol/L NaOH solution at 80 °C. The concentrations of K^+ is shown in (A) and the concentrations of Na^+ is shown in (B).

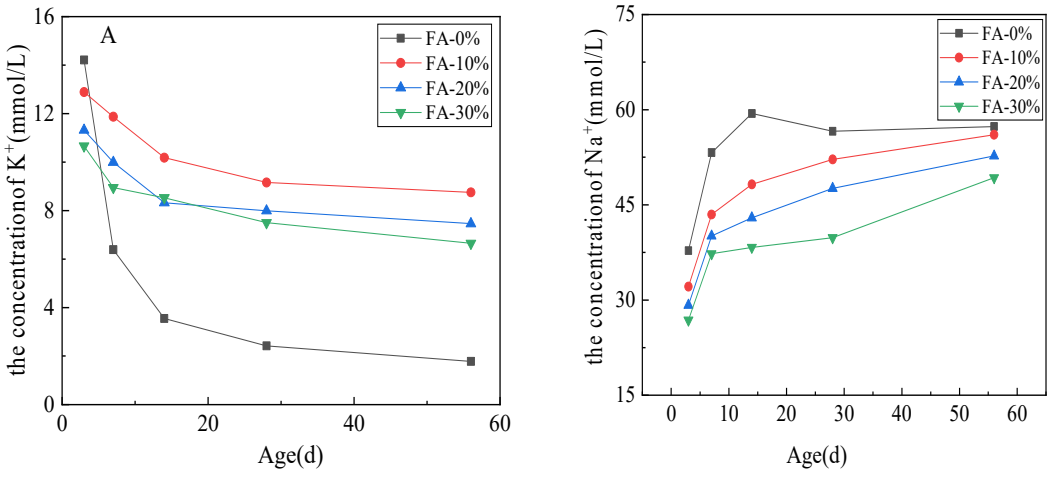

Figure 9. Effect of fly ash on the concentrations of K^+ and Na^+ in the pore solution (80 °C, 1 mol/L NaOH): (**A**) the concentrations of K^+ and (**B**) the concentrations of Na^+.

Figure 9 reveals that, as the amount of fly ash increased, the concentrations of K^+ and Na^+ in the pore solution decreased. Regardless of whether the sample was pulverized or not and mixed with fly ash, the concentration of K^+ ions in the pore solution gradually decreases and the concentration of Na^+ ions increases with the increasing curing time. Increasing the amount of fly ash slows the migration rates of Na^+ and K^+ to the cement paste in the curing solution. The ionic migration rate of the cement

paste without fly ash was the fastest. The concentration of $[K^+ + Na^+]$ in the pore solution was close to 0.063 mol/L at 14 days, but the concentration of $[K^+ + Na^+]$ in the pore solution with 30% fly ash was only 0.055 mol/L at 56 days. There was still a significant difference between the cement paste with fly ash and cement paste without fly ash, which was not offset by the external alkali content. It can be seen that adding fly ash delays the ionic migration and exchange speed of the pore solution to the curing solution.

The pore structure is an important component of the concrete microstructure. Manmohan [25] divided the pores in concrete into four sizes: <4.5, 4.5–50, 50–100, and >100 nm. Mehta believed that only pores larger than 100 nm will affect the strength and permeability of concrete. We tested the effect of fly ash on the pore structure of the cement paste in the concrete microbars, in order to analyze the effect of fly ash on ionic migration. Figure 10 shows the pore volume and pore diameter distributions of the cement paste in the concrete microbars cured for 56 days in 1 mol/L NaOH solution at 80 °C. The porosity of cement paste in the concrete microbars is shown in (A) and the pore size distribution of cement paste in the concrete microbars is shown in (B).

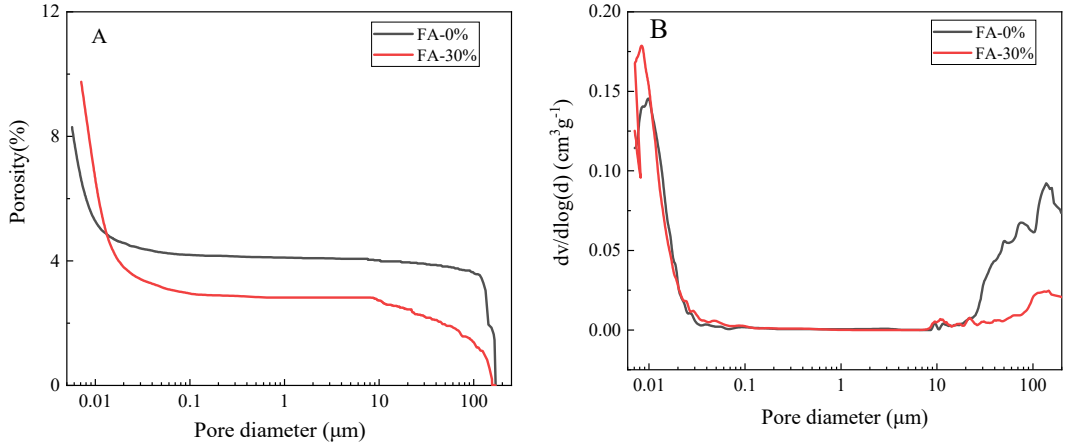

Figure 10. Pore structure of cement paste cured in 1 mol/L NaOH at 80 °C: (**A**) the porosity of cement paste in the concrete microbars and (**B**) the pore size distribution of cement paste in the concrete microbars.

Adding fly ash increased the porosity of the cement paste, reduced the harmful pores larger than 100 nm and increased the amount of micropores, effectively refining the pore structure. The porosity increased from 8% to 10% when using 30% fly ash. According to Manmohan [25], adding fly ash makes the structure of concrete microbars more compact. Fly ash not only reduces the content of the large pores, but also increases the content of small pores; thus, the pore structure of the cement paste becomes more compact, the permeability of the cement paste decreases, and the ionic migration speed becomes slower.

3.4.3. Polarizing Microscope and Stereomicroscope Analysis

The thin sections of the concrete microbars cured in NaOH solutions were observed by polarizing microscopy, as shown in Figure 11. From the figure, we can see the crack characteristics of the concrete prepared with the SJW and BFL8 aggregates in the NaOH solution. The cracks were created inside the rock and extended into the cement paste. We can see many different sizes of dolomite crystals distributed at the crack. Meanwhile, no ASR gel was found in the crack. Therefore, these cracks are expansion cracks, mainly due to the ACR.

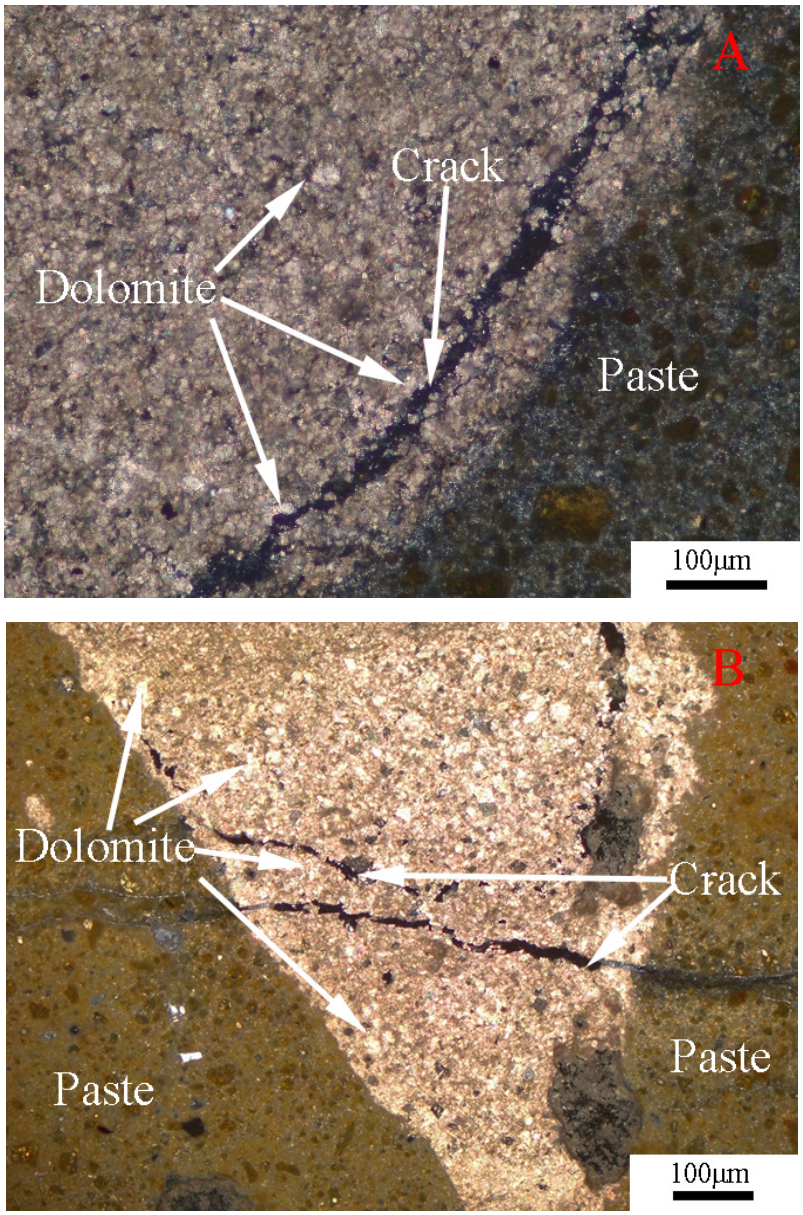

Figure 11. Thin section of the concrete microbars cured in NaOH solution for 180 days: (**A**) concrete microbars prepared with SJW; and (**B**) concrete microbars prepared with BFL8.

The expansion cracks of the concrete microbars cured in 1 mol/L NaOH solution were examined by stereomicroscope analysis, as shown in Figure 12. From the figure, we can see that cracks appeared in the concrete microbars without fly ash. However, the concrete microbars mixed with 30% fly ash had only some fine cracks and even no cracking. This indicates that the addition of fly ash can significantly reduce the cracking in concrete microbars.

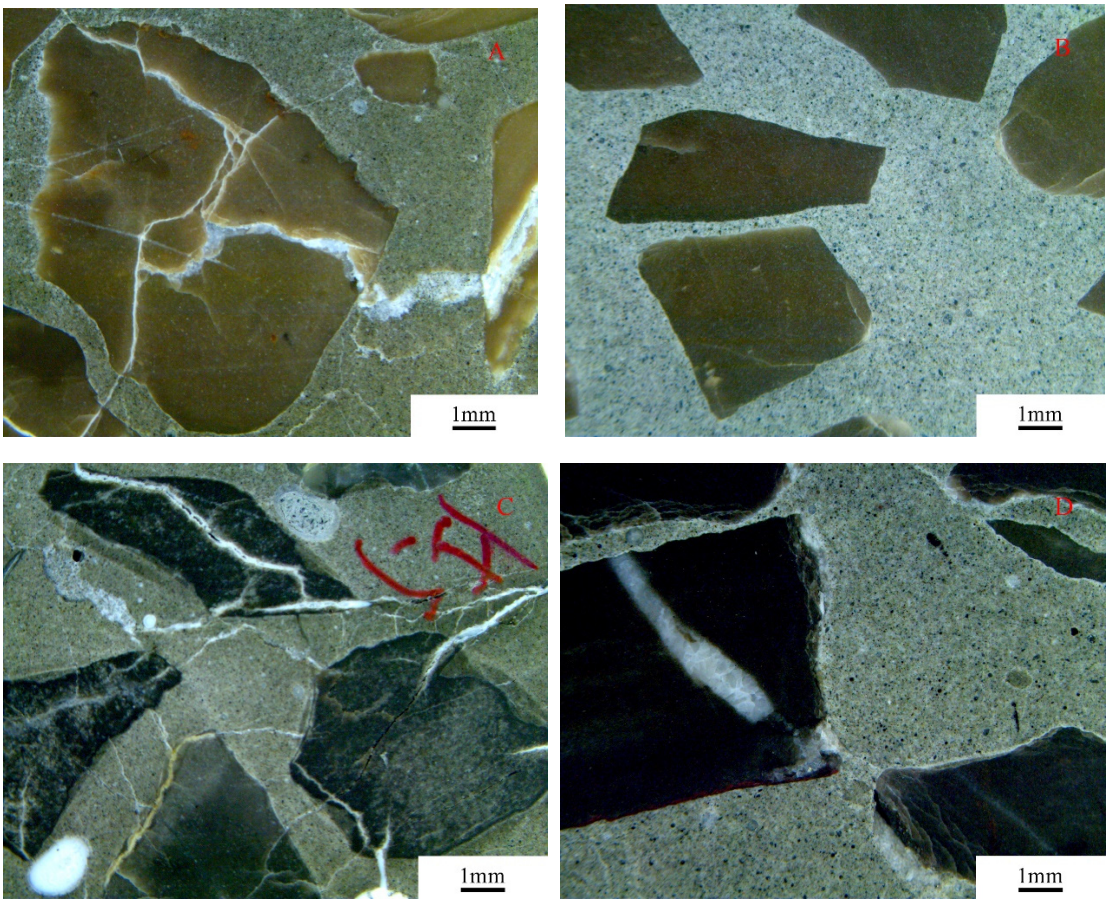

Figure 12. Expansion cracks of concrete microbars prepared with the dolomitic aggregate cured in NaOH solution for 56 days: (**A**) BFL8; (**B**) BFL8 with 30% fly ash; (**C**) SJW; and (**D**) SJW with 30% fly ash.

The above analysis shows that the dolomite in the rock had undergone a dolomitization reaction, and the cracks of the concrete microbars prepared with BFL8 and SJW were in dolomite-rich areas. Due to the fly ash refining the pore structure of the cement paste and reducing the migration rate of the alkali in the curing solution to the interior of the concrete microbars, as the content of fly ash increased, the concentration of K^+ and Na^+ and the pH value in the pore solution gradually decreased. This made the ACR in the rock slower, the cracks reduce, and the ACR expansion to be inhibited.

4. Conclusions

In this experiment, concrete microbars and concrete prisms made of dolomite aggregates, fly ash, and cement were used to systematically investigate the short- and long-term effects of fly ash on the ACR and to investigate the influence of fly ash on the expansion of dolomite aggregates. From the physical macro-measurements and microstructure analyses, the following main conclusions can be drawn:

Increasing the content of fly ash in concrete microbars and concrete prisms can considerably decrease the expansion rate due to the ACR. In comparison with adding 10% and 20% fly ash, concrete microbars prepared with 30% fly ash exhibited a greatly reduced expansion rate. According to the expansion rates of concrete microbars, when the alkali equivalent (equivalent Na_2Oeq) of the cement was 1.0%, for low-reactivity aggregates (such as BFL8), adding 30% fly ash could inhibit the expansion due to the ACR. However, when adding 30% fly ash to moderately reactive aggregates, such as SJW, although the expansion rate decreased, it did not decrease to less than 0.1% and cracking still occurred.

The polarizing microscope and stereomicroscope analysis results indicated that the cracks were expansion cracks, and the expansion was mainly due to the ACR. Adding 30% fly ash could significantly reduce the cracking in concrete microbars.

Through the analysis of the K^+ and Na^+ concentrations, the pH value, the ionic migration of the cement paste pore solution, and the pore structure, the main mechanism of fly ash inhibiting the ACR is that fly ash refines the pore structure of the cement paste, and the alkali migration rate in the curing solution to the interior of the concrete microbars is reduced. As the content of fly ash increases, the concentration of K^+ and Na^+ and the pH value in the pore solution gradually decrease. This causes the ACR in the rock to slow, the cracking to reduce, and the ACR expansion to be inhibited.

Author Contributions: Conceptualization, X.R. and M.D.; methodology, X.R.; software, X.R.; validation, X.R.,W.L., Z.M., and M.D.; formal analysis, X.R.; investigation, X.R.; resources, X.R., W.L. and Z.M.; data curation, X.R.; writing—Original draft preparation, X.R.; writing—review and editing, X.R.; visualization, X.R.; supervision, M.D.; project administration, M.D.; funding acquisition, M.D. All authors have read and agreed to the published version of the manuscript.

Funding: This work was funded by the National Key Research and Development Project (2016YFB0303601-2) and the Priority Academic Program Development of Jiangsu Higher Education Institutions (PAPD).

Acknowledgments: The authors gratefully acknowledge the assistance from Jun Wang, Pengcheng Yu and Huan Yuan from NJTECH, and the staff from State Key Laboratory of Materials-Oriented Chemical Engineering.

Conflicts of Interest: The authors declare no conflict of interest.

References

1. Stanton, T.E. Expansion of concrete through reaction between cement and aggregate. *Proc. Asce* **1940**, *6*, 1781–1811.
2. Gillott, J.E. Mechanism and kinetics of expansion in the alkali-carbonate rock reaction. *Can. J. Earth Sci.* **1964**, *1*, 121–145. [CrossRef]
3. Tang, M.; Liu, Z.; Han, S. Mechanism of alkali-carbonate reaction. In Proceedings of the 7th ICAAR in Concrete, Ottawa, ON, Canada, 18–22 August 1986; pp. 275–279.
4. Deng, M.; Mingshu, T. Mechanism of dedolomitization and expansion of dolomitic rocks. *Cem. Concr. Res.* **1993**, *23*, 1397–1408.
5. Tong, L.; Tang, M. Expansion mechanism of alkali-dolomite and alkali-magnesite reaction. *Cem. Concr. Compos.* **1999**, *21*, 361–373. [CrossRef]
6. Katayama, T.; Tagami, M.; Sarai, Y. Alkali-aggregate reaction under the influence of deicing salts in the Hokuriku district, Japan. *Mater. Charact.* **2004**, *53*, 105–122. [CrossRef]
7. Katayama, T. How to identify carbonate rock reactions in concrete. *Mater. Charact.* **2004**, *53*, 85–104. [CrossRef]
8. Katayama, T. The so-called alkali-carbonate reaction (ACR)—Its mineralogical and geochemical details, with special reference to ASR. *Cem. Concr. Res.* **2010**, *40*, 643–675. [CrossRef]
9. Chen, X.; Yang, B.; Mao, Z. The expansion cracks of dolomitic aggregates cured in TMAH solution caused by alkali–carbonate reaction. *Materials* **2019**, *12*, 1228. [CrossRef]
10. Chen, B.; Deng, M.; Lan, X. Behaviors of reactive silica and dolomite in tetramethyl ammonium hydroxide solutions. In Proceedings of the 15th international conference on Alkali-aggregate reactions in concrete, St Paul, Brazil, 3–7 July 2016; pp. 3–7.
11. Yuan, H.; Deng, M.; Chen, B. Expansion of dolomitic rocks in TMAH and NaOH solutions and its root causes. *Materials* **2020**, *13*, 308. [CrossRef] [PubMed]
12. Lindgård, J.; Andiç-Çakır, Ö.; Fernandes, I. Alkali–silica reactions (ASR): literature review on parameters influencing laboratory performance testing. *Cem. Concr. Res.* **2012**, *42*, 223–243. [CrossRef]
13. Kawabata, Y.; Yamada, K. The mechanism of limited inhibition by fly ash on expansion due to alkali–silica reaction at the pessimum proportion. *Cem. Concr. Res.* **2017**, *92*, 1–15. [CrossRef]
14. Thomas, M. The effect of supplementary cementing materials on alkali-silica reaction: A review. *Cem. Concr. Res.* **2011**, *41*, 1224–1231. [CrossRef]

15. Joshaghani, A. The effect of trass and fly ash in minimizing alkali–carbonate reaction in concrete. *Constr. Build. Mater.* **2017**, *150*, 583–590. [CrossRef]
16. Shehata, M.H.; Jagdat, S.; Rogers, C. Long-term effects of different cementing blends on alkali-carbonate reaction. *Aci Mater. J.* **2017**, *114*, 661–672. [CrossRef]
17. Min, D.; Mingshu, T. Measures to inhibit alkali-dolomite reaction. *Cem. Concr. Res.* **1993**, *23*, 1115–1120. [CrossRef]
18. AAR, R.R. Detection of potential alkali-reactivity of aggregates-The ultra-accelerated mortar-bar test. *Mater. Struct.* **2000**, *33*, 226.
19. Sommer, H.; Nixon, P.J.; Sims, I. AAR–5: Rapid preliminary screening test for carbonate aggregates. *Mater. Struct.* **2005**, *38*, 787–792. [CrossRef]
20. ASTM C1293–08: Standard Test Method for Determination of Length Change of Concrete Due To Alkali–Silica Reaction. Available online: https://books.google.com.hk/books?id=9ILMBQAAQBAJ&pg=PA8&lpg=PA8&dq=20.%09ASTM+C1293%E2%80%9308:+Standard+test+method+for+determination+of+length+change+of+concrete+due+to+alkali%E2%80%93silica+reaction.&source=bl&ots=VxAaWxR3Oj&sig=ACfU3U2hRlpMOExB6rYk5bs8pXWL_UuNrA&hl=en&sa=X&redir_esc=y&hl=zh-CN&sourceid=cndr#v=onepage&q=20.%09ASTM%20C1293%E2%80%9308%3A%20Standard%20test%20method%20for%20determination%20of%20length%20change%20of%20concrete%20due%20to%20alkali%E2%80%93silica%20reaction.&f=false (accessed on 4 June 2020).
21. French, W.J. Concrete petrography: A review. *Q. J. Eng. Geol.* **1991**, *24*, 17–48. [CrossRef]
22. Deng, M.; Tang, M.S. Mechanism and prevention of alkali-dolomite reaction. *J. Nanjing Univ. Chem. Technol.* **1998**, *20*, 1–7.
23. Dunstan, E.R. The chemistry of alkali-aggregate reactions. *Cem. Concr. Aggreg.* **1981**, *3*, 101–104.
24. Xu, G.; Tian, Q.; Miao, J. Early-age hydration and mechanical properties of high-volume slag and fly ash concrete at different curing temperatures. *Constr. Build. Mater.* **2017**, *149*, 367–377. [CrossRef]
25. Mehta, P.K. Study on blended portland cements containing santirin earth. *Cem. Concr. Res.* **1981**, *11*, 507–518. [CrossRef]